SUPPLEMENTAL INFORMATION

Therapeutic mTorc1 inhibition restricts inflammation-associated gastrointestinal tumorigenesis in mice

Stefan Thiem, Thomas P. Pierce, Michelle Palmieri, Tracy L. Putoczki, Michael Buchert, Adele Preaudet, Ryan O. Farid, Chris Love, Bruno Catimel, Zhengdeng Lei, Steve Rozen, Veena Gopalakrishnan, Fred Schaper, Michael Hallek, Alex Boussioutas, Patrick Tan, Andrew Jarnicki and Matthias Ernst

Supplemental Data

Thiem *et al*., Supplemental Figure 1

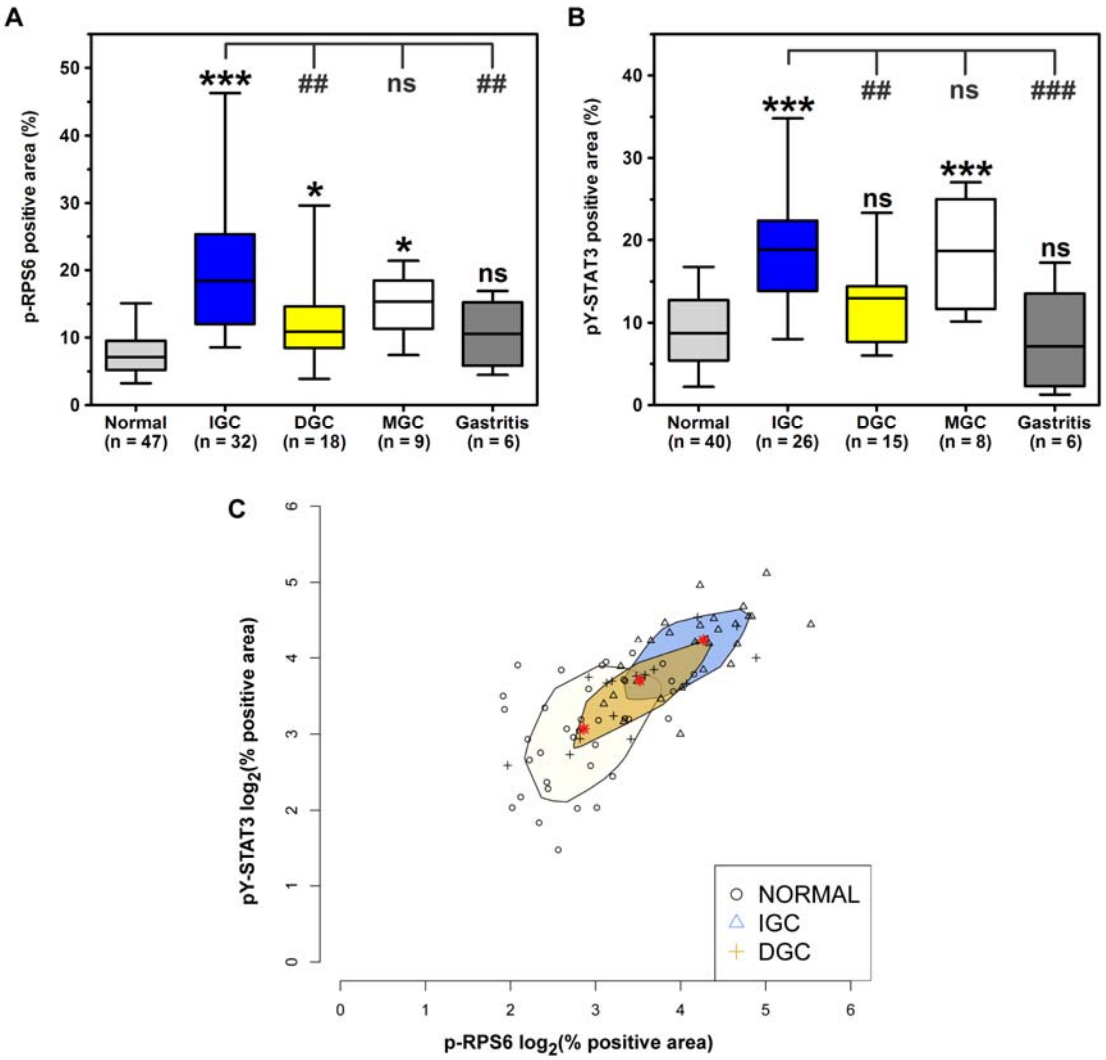

Figure S1. Co-activation of mTORC1 and STAT3 in human GC.

(A-B) Quantification of the p-RPS6 and pY-STAT3 immunostaining on human GC biopsy sections (*Figure 1A*; IGC = intestinal-type GC, DGC = diffuse-type GC, MGC = mixed GC). The box-and-whisker plot shows the percentage of the p-RPS6 positive area (**A**) and the pY-STAT3 positive area (**B**) relative to the total tissue area. The line in the box represents the median, and the span of the box represents the 25% range of the data. The top and bottom whiskers of the plot indicate maximum and minimum values including all outliers. *P* values were calculated by One-Way Anova (compared to Normal: * $P<0.05$, *** $P<0.001$; compared to IGC: $^{\#\#}$ $P<0.01$, $^{\#\#\#}$ $P<0.001$; ns = not significant).

(C) Bagplot representation of the quantified p-RPS6 and pY-STAT3 immunostainings on human GC sections. The $\log_2$-transformed percentage of positively stained tissue area is shown for Normal, IGC and DGC (for clarity MGC and Gastritis data are not displayed in the bagblot). The red asterisk highlighted in the middle of each 'bag' represents the estimated two-dimensional median and the points within the enclosed section represent 50% of all points for each respective GC subtype. The bagblot was displayed using the R 'aplpack' package. *P* values (Pr(>F) values) were calculated using a pairwise multivariate analysis of variance (MANOVA) test.

Thiem *et al*., Supplemental Figure 2

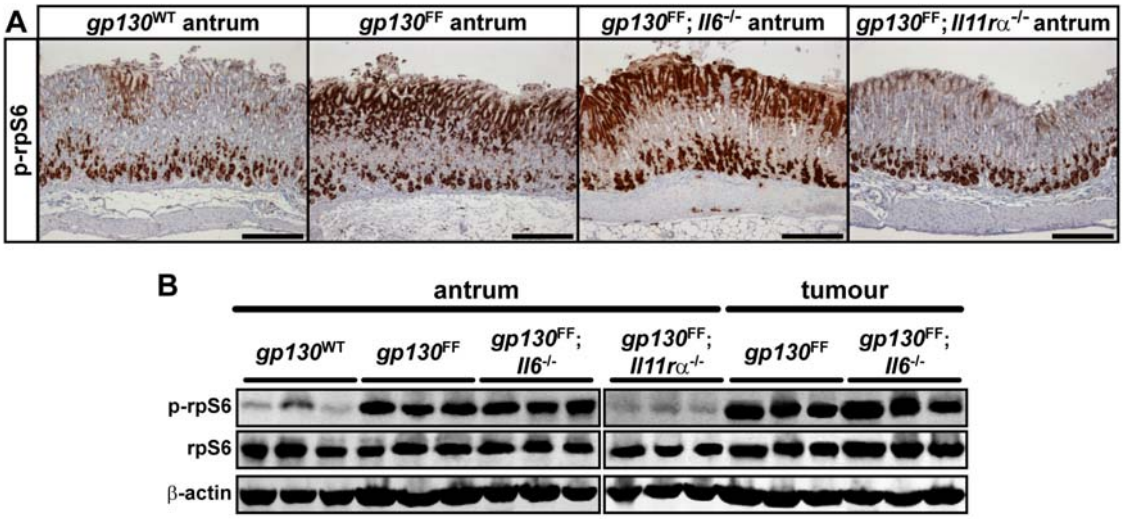

Figure S2. Basal mTorc1 activity in the stomach of *gp130*^{FF} compound mutant mice.

(A) Representative immunostaining for p-rpS6 on unaffected antrum sections from 10 week old mice with the indicated genotype. Scale: 200 µm.

(B) Immunoblot analysis for p-rpS6 with each lane corresponding to the protein lysate of unaffected antrum or pooled tumours from an individual mouse with the indicated genotype.

Thiem *et al*., Supplemental Figure 3

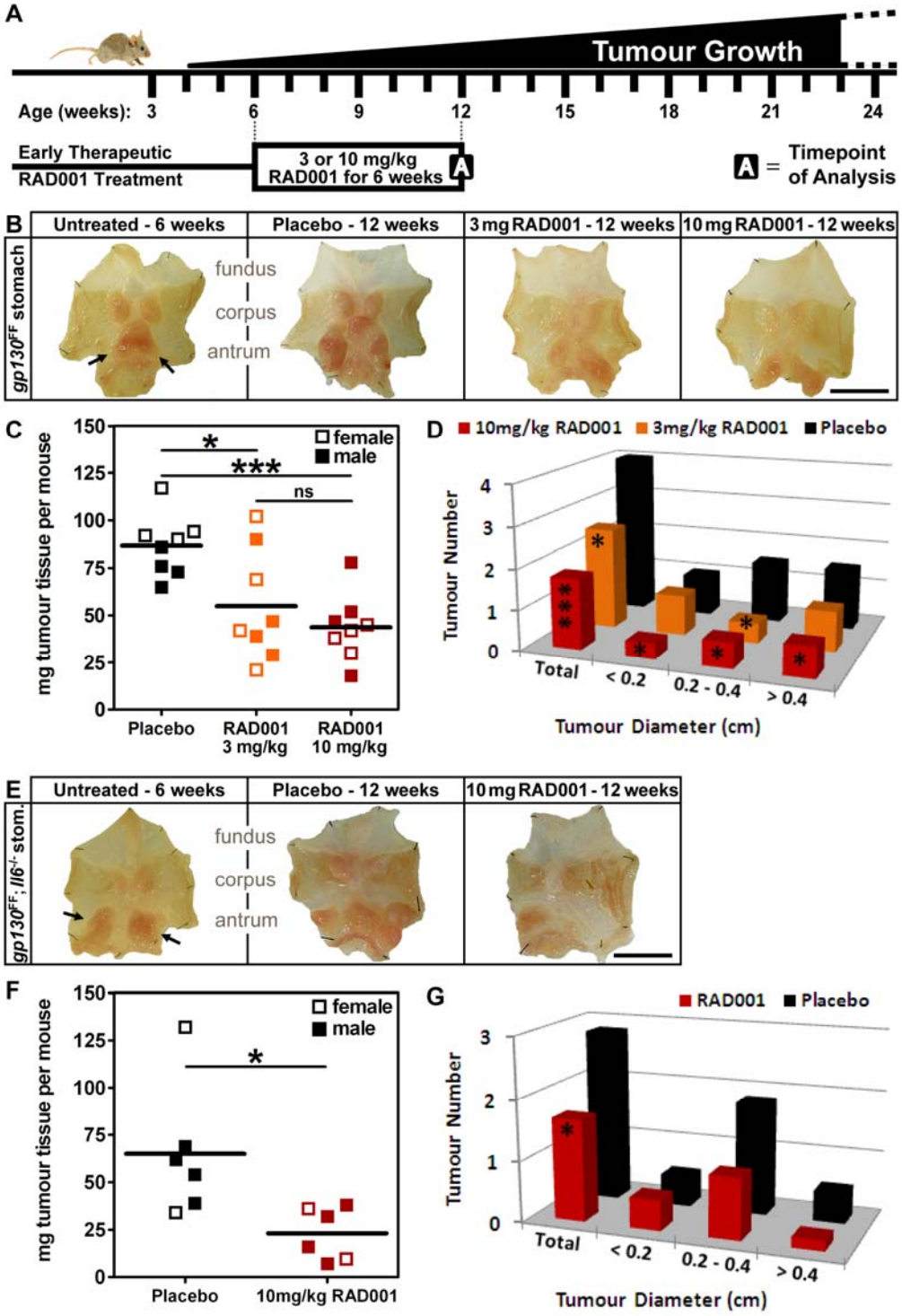

Figure S3. Therapeutic RAD001 treatment of 6 week old *gp130*^{FF} and *gp130*^{FF}; *Il6*$^{-/-}$ mice.

(A) Schematic illustration of spontaneous gastric tumorigenesis in *gp130*^{FF} and *gp130*^{FF}; *Il6*$^{-/-}$ mice and the RAD001 treatment protocol.

(B, E) Whole-mount photographs of representative stomachs from *gp130*^{FF} (**B**) or *gp130*^{FF}; *Il6*$^{-/-}$ (**E**) mice at the beginning and end of the RAD001 treatment period. Scale: 1 cm. The arrows indicate established gastric tumours prior to commencing RAD001 therapy.

(C-D, F-G) For each individual mouse (*gp130*^{FF}: n=8 (**C-D**), *gp130*^{FF}; *Il6*$^{-/-}$: n=6 (**F-G**) per cohort), the combined mass of resected tumours was determined (**C, F**) and individual tumours were enumerated and classified according to their size (**D, G**). Horizontal lines refer to mean values (* P<0.05, *** P<0.001, ns = not significant).

Thiem *et al*., Supplemental Figure 4

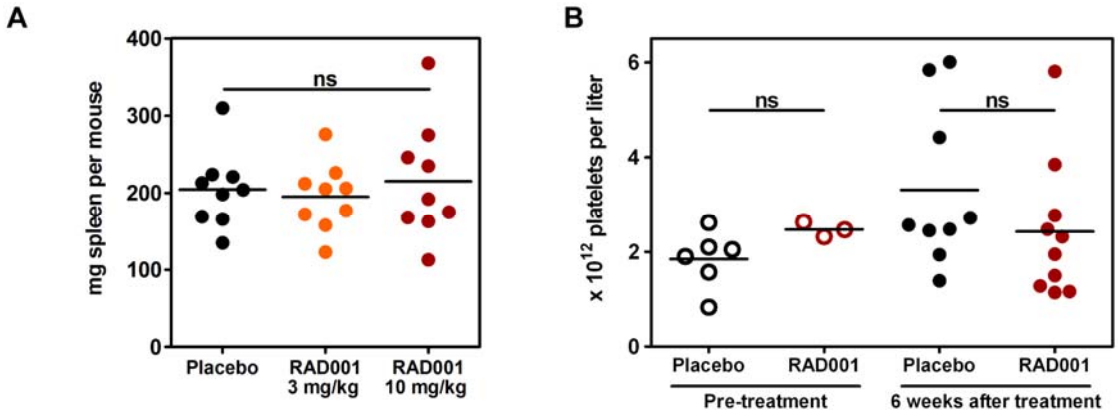

Figure S4. RAD001 has no impact on splenomegaly and thrombocytosis in *gp130*^{FF} mice.

(A) Spleen mass per individual placebo- or RAD001-treated mouse (n≥9 per cohort). Horizontal lines refer to mean values (ns = not significant).

(B) Platelet count per individual mouse (n≥9 per cohort) at the beginning and end of the RAD001 treatment period. Horizontal lines refer to mean values (ns = not significant).

Thiem *et al*., Supplemental Figure 5

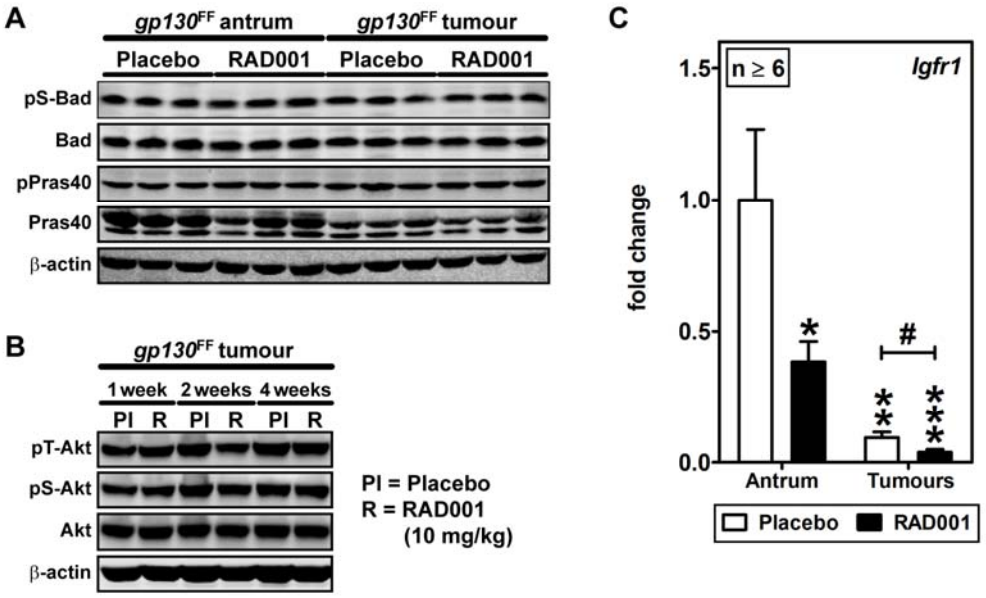

Figure S5. Tumorigenesis in *gp130*^{FF} mice requires continuous mTorc1 activity.

(A) Immunoblot analysis of unaffected antrum and pooled tumours from individual mice at the end of the RAD001 (10 mg/kg) treatment period.

(B) Immunoblot analysis of pooled tumours from individual mice collected following 1, 2 and 4 weeks of RAD001 treatment (10 mg/kg).

(C) qRT-PCR analysis of Insulin-like growth factor receptor (*Igfr*) 1 in the unaffected antrum and pooled tumours from 19 week old *gp130*^{FF} mice (n≥6 per cohort) which were treated for the last 6 weeks with 10 mg/kg RAD001. Data were normalized to 18S rRNA expression and are expressed as mean fold change ± SEM compared to the antrum sample of placebo-treated mice (* P<0.05, ** P<0.01, *** P<0.001; $^{\#}$ P<0.05 compared to the tumour sample of placebo-treated mice).

Thiem *et al*., Supplemental Figure 6

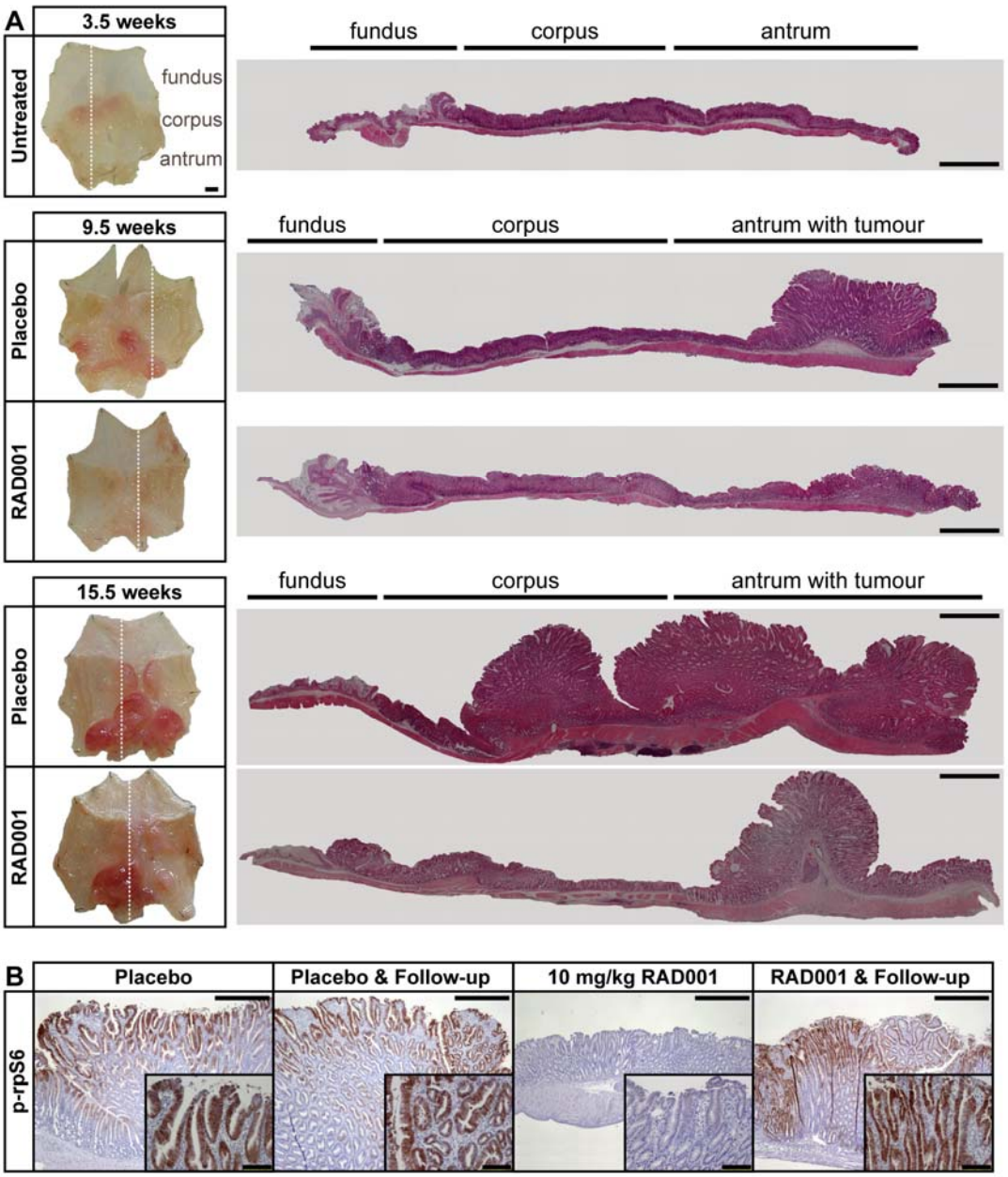

Figure S6. Tumorigenesis in *gp130*^{FF} mice requires continuous mTorc1 activity.

(A) Whole-mount photographs of representative stomachs from *gp130*^{FF} mice of the indicated age and treatment. The pinned-out stomachs were cut along the dotted line and stained with haematoxylin and eosin for histological analysis. Scale: 2 mm.

(B) Representative immunostaining for p-rpS6 on tumour sections from RAD001- and placebo-treated *gp130*^{FF} mice sacrificed after the RAD001 treatment period or after an additional 6 week treatment-free follow-up period. Scale: 500 µm (*insets*: 100 µm).

Thiem *et al*., Supplemental Figure 7

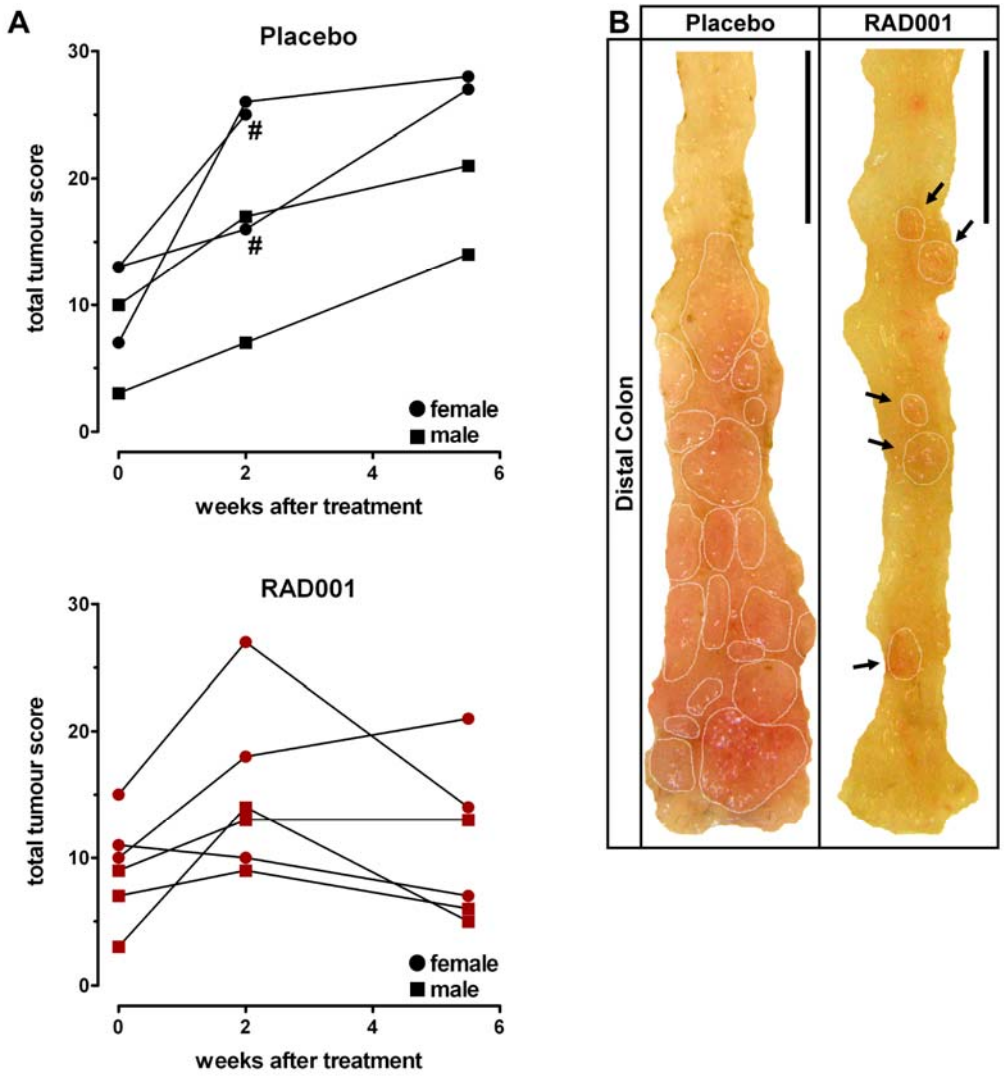

Figure S7. RAD001 suppresses tumour growth in a model of colitis-associated cancer (CAC).

(A) Tumour scores of individual CAC-challenged wild-type mice (n≥5 per cohort) were obtained by endoscopy (1) at the indicated time points during RAD001 treatment. In some mice (#), the size of a single tumour prevented complete endoscopic analysis.

(B) Whole-mount photographs of representative distal colons collected at the end of the 6 week treatment period with RAD001. Scale: 1 cm. Tumours are encircled and arrows indicate the remaining small tumours in the distal colon of RAD001-treated mice.

Thiem *et al*., Supplemental Figure 8

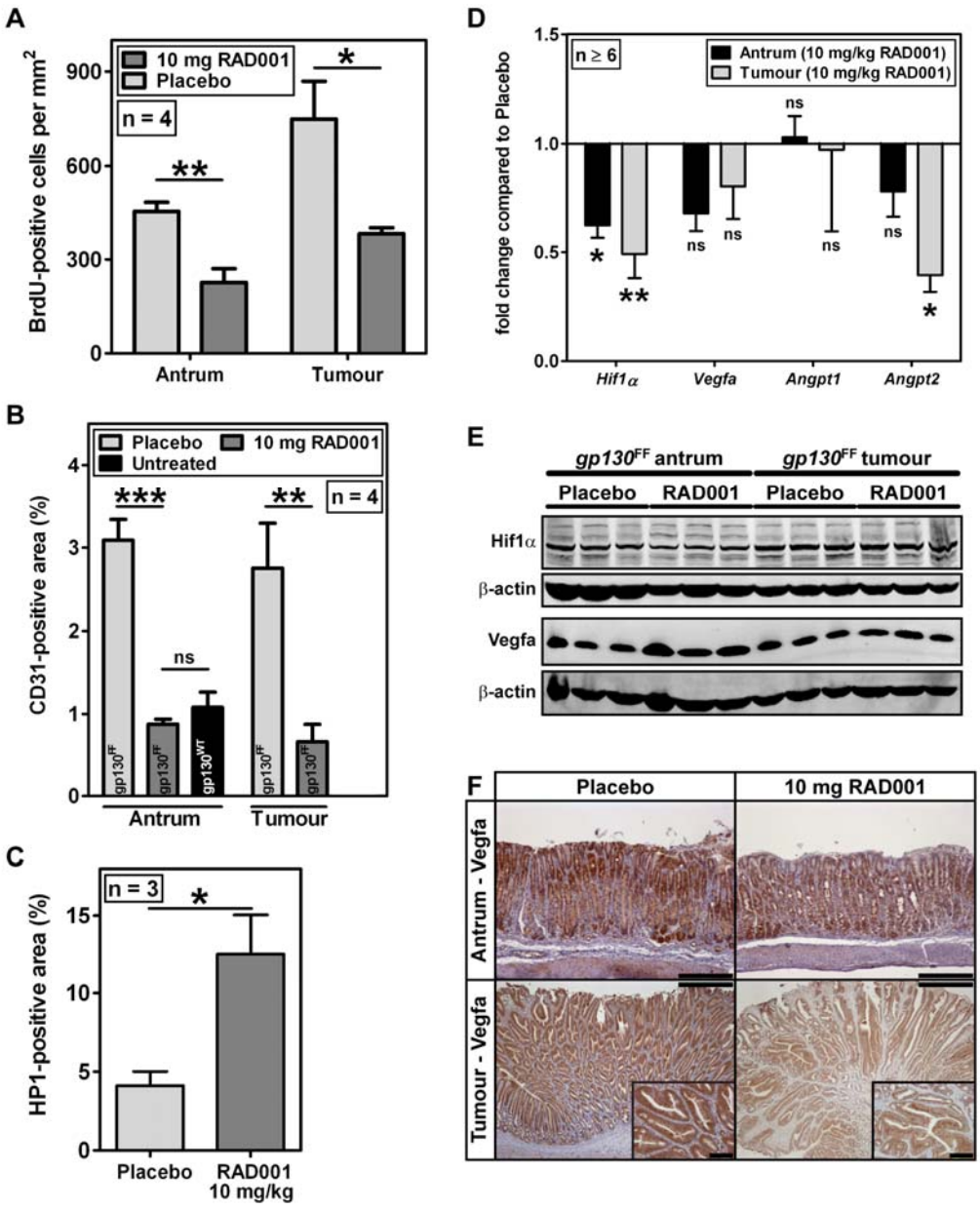

Figure S8. RAD001 treatment decreases tumour cell proliferation and induces tissue hypoxia.

(A) Quantification of BrdU-positive cells per mm^2 of antral and tumour tissue area represented as mean ± SEM (* *P*<0.05, ** *P*<0.01).

(B-C) Quantification of areas stained positive for CD31 (**B**) or HP1 (**C**) represented as mean ± SEM (* *P*<0.05, ** *P*<0.01, *** *P*<0.001).

(D) qRT-PCR analysis of hypoxia-associated genes in the unaffected antrum and pooled tumours from 19 week old *gp130*^{FF} mice (n≥6 per cohort) which were treated for the last 6 weeks with 10 mg/kg RAD001. Data were normalized to 18S rRNA expression and are expressed as mean fold change ± SEM compared to placebo-treated mice (*P<0.05, ** P<0.01, ns = not significant).

(E) Immunoblot analysis of unaffected antrum and pooled tumours from individual 19 week old *gp130*^{FF} mice which were treated for the last 6 weeks with 10 mg/kg RAD001.

(F) Representative immunostaining for Vegfa on antrum and tumour sections from 19 week old *gp130*^{FF} mice which were treated for the last 6 weeks with 10 mg/kg RAD001. Scale: 500 µm (*insets*: 100 µm).

Thiem *et al*., Supplemental Figure 9

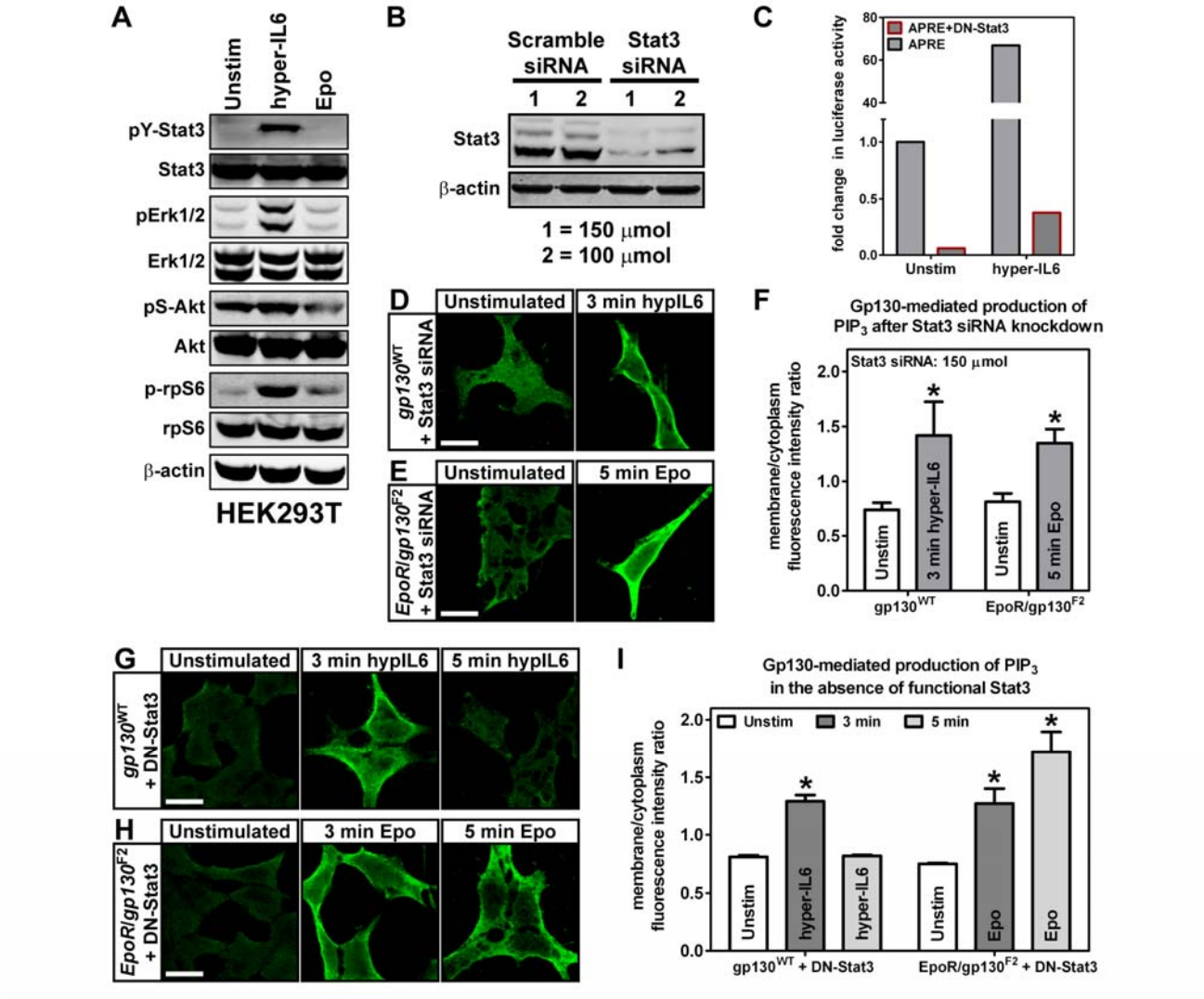

Figure S9. Gp130-mediated PIP_3 production occurs independently of Stat3 activity.

(A-B) Immunoblot analysis of lysates from 293T cells that were serum-starved and stimulated for 60 min with 100 ng/ml Hyper-IL6 or 50 U/ml Epo (**A**), or were transfected with scramble or Stat3 siRNA (**B**). Note: Naïve 293T cells do not respond to Epo (**A**).

(C) Transcriptional Stat3 activity was monitored in 293T cells transfected with the Stat3 reporter construct APRE-luciferase (APRE) alone or together with a plasmid encoding dominant-negative Stat3 (DN-Stat3). Luciferase activity was assessed 48 hours after transfection in unstimulated or Hyper-IL6 stimulated (100 ng/ml) cells. Results are expressed as mean fold change in luciferase activity.

(D-I) Formation of PIP_3 was monitored as an indicator of PI3K activity by immunofluorescent staining using the PIP_3-specific GST–GRP1PH probe. Stainings were performed 72 hours after Stat3 siRNA (150 µmol) transfection (**D-F**) or 48 hours after transfection of DN-Stat3 (**G-I**). The representative images show naïve 293T cells (**D, G**) or cells transiently expressing the chimeric EpoR/$gp130^{F2}$ receptor (**E, H**). Cells were stimulated for the indicated time with 100 ng/ml Hyper-IL6 (**D, G**) or 50 U/ml Epo (**E, H**). Images were then used for cell segmentation analysis and quantification with MetaMorph software (**F, I**). For each time point a total of 100-200 cells were analysed and results are depicted as mean ± SEM (* P<0.05 compared to unstimulated isogenic cells). Scale: 10 µm.

Thiem *et al*., Supplemental Figure 10

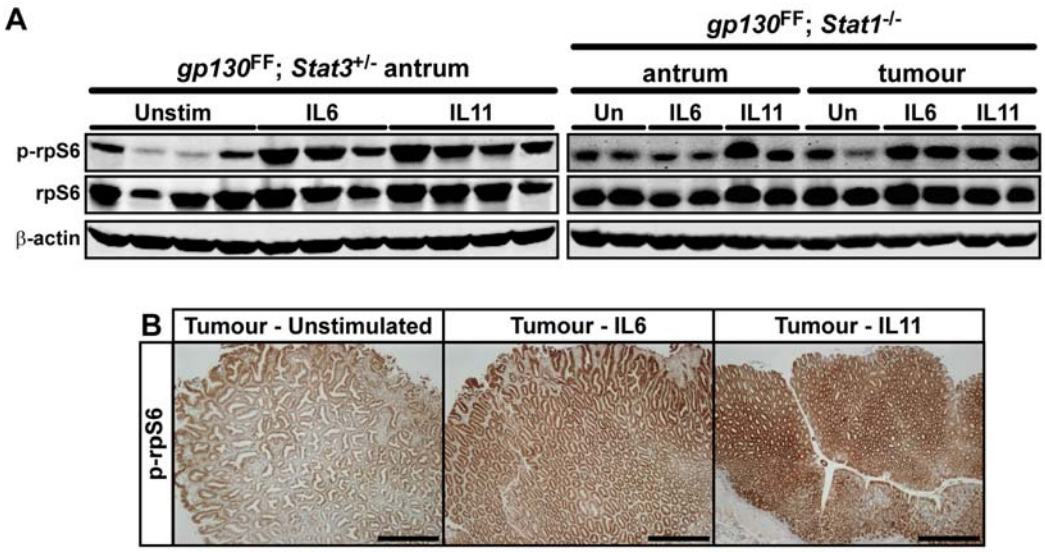

Figure S10. Gp130-mediated mTorc1 activation occurs independently of Stat3 and Stat1.

(A) Immunoblot analysis of unaffected antrum and pooled tumours from individual 10 week old *gp130*^{FF} compound mutant mice collected 60 min after a single i.p. injection of 5 µg of IL6 or IL11.

(B) Representative immunostaining for p-rpS6 on sections of gastric tumours from 10 week old *gp130*^{FF}; *Stat1*$^{-/-}$ mice collected 60 min after a single i.p. injection of 5 µg of IL6 or IL11. Scale: 500 µm.

Thiem *et al*., Supplemental Figure 11

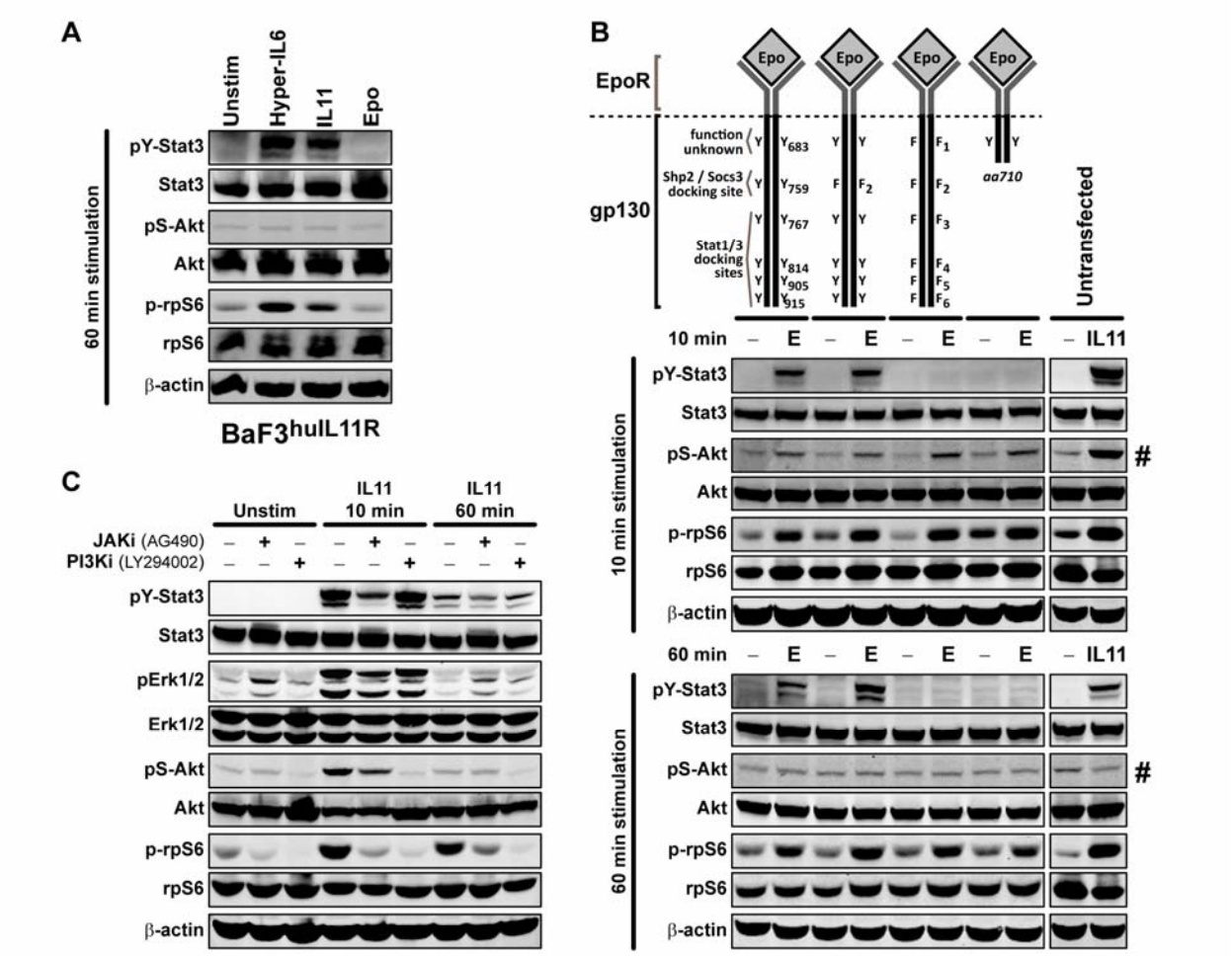

Figure S11. Gp130-mediated activation of the PI3K/Akt/mTorc1 pathway requires Janus kinase activity.

(A) Immunoblot analysis of BaF3 cells stably expressing the human, ligand-binding IL11α receptor chain (BaF3^{huIL11R}). Cells were IL3-starved and stimulated for 60 min with either Hyper-IL6 (100 ng/ml), IL11 (100 ng/ml) or Epo (50 U/ml). Note: BaF3^{huIL11R} cells do not respond to Epo stimulation.

(B) Immunoblot analysis of naïve BaF3^{huIL11R} cells or of cells expressing the indicated chimeric EpoR/gp130 receptor (*top panel*). IL3-starved cells were analysed 10 min (*middle panel*) and 60 min (*bottom panel*) after stimulation with Epo (E; 50 U/ml) or IL11 (100 ng/ml). Note: Akt (#) is transiently phosphorylated, while rpS6 and Stat3 remain phosphorylated 60 min after cytokine stimulation.

(C) Immunoblot analysis of naïve BaF3^{huIL11R} cells that were stimulated with IL11 (100 ng/ml) for the indicated time. A subset of cultures were pre-treated with the pan-Jak inhibitor AG490 (75 μM) or the PI3K inhibitor LY294002 (25 μM) 60 min prior to IL11 stimulation.

Thiem *et al*., Supplemental Figure 12

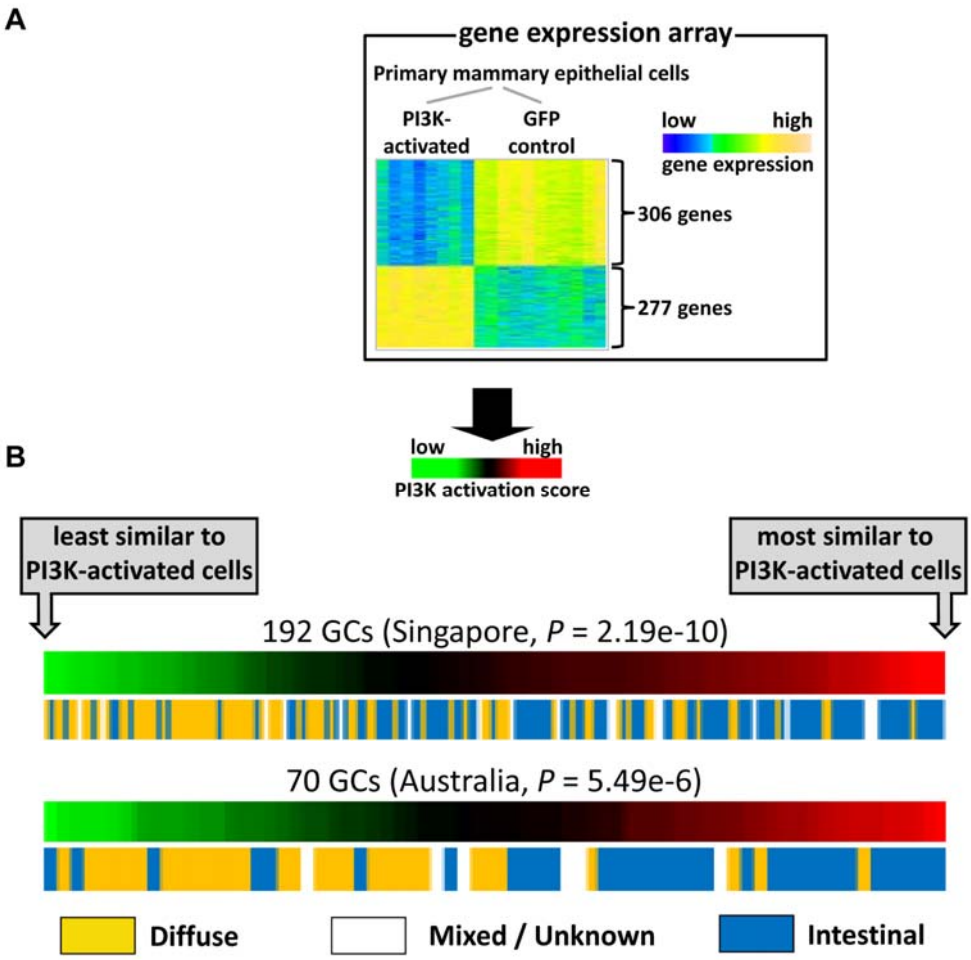

Figure S12. Correlation between gene expression profiles of PI3K-activated cells and human GC.

(A-B) Correlation of the gene expression profiles between PI3K-activated primary mammary epithelial cells and human GC. (**A**) Heat map of differentially expressed genes between PI3K-activated and normal (GFP control) mammary epithelial cells. (**B**) The human orthologs of these genes were used to calculate a human "PI3K activation score" for individual expression signatures of GC biopsies collected in Singapore or Australia. The panels depict the correlation between the "PI3K activation score" of each biopsy and their histological classification according to Lauren. *Also refer to Table S2*.

Supplemental Methods

MATERIALS

Antibodies for immunoblot analysis

Primary antibodies were against pY-Stat3 (Tyr-705; Cell Signaling #9145), pS-Stat3 (Ser-727; Cell Signaling #9134), Stat3 (Cell Signaling #4904), p-rpS6 (Ser-240/244; Cell Signaling #2215), rpS6 (Cell Signaling #2217), pT-4EBP1 (Thr-33/45; Cell Signaling #2855), pS-4EBP1 (Ser-64; Cell Signaling #9451), 4EBP1 (Cell Signaling #9452), pS-Akt (Ser-473; Cell Signaling #4058), pT-Akt (Thr-308; Cell Signaling #9275), Akt (Cell Signaling #9272), pMek1/2 (Ser-217/221; Cell Signaling #9154), pErk1/2 (p44/42 MAPK, Thr-202/Tyr-204; Cell Signaling #9101), Erk1/2 (Cell Signaling #4695), pPras40 (Thr-246; Cell Signaling #2640), Pras40 (Cell Signaling #2610), pS-Bad (Ser-112; Cell Signaling #9296), Bad (Cell Signaling #9292), cleaved (activated) Caspase-9 (Cell Signaling #9504), cleaved (activated) Caspase-3 (R&D Systems #AF835), Hif1α (Abcam #ab2185), Vegfa (Santa Cruz #152) and β-actin (Sigma #A2066).

Antibodies for immunohistochemical analysis

Primary antibodies were against pY-Stat3 (Tyr-705; Santa Cruz #7993), p-rpS6 (Ser-240/244; Cell Signaling #2215), pErk1/2 (p44/42 MAPK, Thr-202/Tyr-204; Cell Signaling #9101), Pten (Cell Signaling #9559), CD31 (BD Biosciences/Pharmingen #553370), cleaved (activated) Caspase-3 (R&D Systems #AF835), Vegfa (Santa Cruz #152), BrdU (BD Biosciences/Pharmingen #555627) and hydroxyprobe-1 (Hypoxyprobe™-1 Kit, Chemicon).

Oligonucleotides for qRT-PCR analysis

All primer pairs were tested for specificity and efficiency. The primer sequences were as follows: *18S rRNA* forward 5'-GTAACCCGTTGAACCCCATT-3', reverse 5'-CCATCCAATCGGTAGTAGCG-3'; *Igfr1* forward 5'-GGGCTGGTTATCATGCTGTAT-3', reverse 5'-CCATTCATCAGGCACGTACA-3'; *Hif1α* forward 5'-GCACCCTAACAAGCCGGGGG-3', reverse 5'-ACCAAGCACGTCATGGGTGGTTTC-3'; *Vegfa* forward 5'-CCAGGCTGCACCCACGACAG-3', reverse 5'-CGGCACACAGGACGGCTTGA-3'; *Angpt1* forward 5'-ATCCCGACTTGAAATACAACTGC-3', reverse 5'- CTGGATGATGAATGTCTGACGAG-3'; *Angpt2* forward 5'-CCTCGACTACGACGACTCAGT-3', reverse 5'-TCTGCACCACATTCTGTTGGA-3'.

Plasmids encoding chimeric EpoR/gp130 receptors

The expression plasmids used for transfection encode different versions of the chimeric human gp130 receptor fused to the extracellular domain of the human erythropoietin receptor (EpoR; 2-4). The plasmids p*EpoR*/*gp130*^{YYYYYY} (EpoR/gp130^{WT}) and p*EpoR*/*gp130*^{YFYYYY} (EpoR/gp130^{F2}) were described previously (2). The plasmids encoding the EpoR/gp130 tyrosine mutant receptors (3) are based on the pRcCMV-ErG(gp130)myc vector and include the following plasmids: p*EpoR*/*gp130*^{FFFFFF}, p*EpoR*/*gp130*^{FFFFFY}, p*EpoR*/*gp130*^{FFFFYF}, p*EpoR*/*gp130*^{FFFYFF}, p*EpoR*/*gp130*^{FFYFFF}, p*EpoR*/*gp130*^{FYFFFF} and p*EpoR*/*gp130*^{YFFFFF}. All plasmids encoding truncated EpoR/gp130 receptors (4) are based on the pcDNA6 vector and include the plasmids p*EpoR*/*gp130*^{trunc710} (truncated from amino acid 710), p*EpoR*/*gp130*^{trunc770} (truncated from amino acid 770) and p*EpoR*/*gp130*^{trunc775} (truncated from amino acid 775). The sequence of all plasmids was verified prior to transfection.

ADDITIONAL METHODS

RNA isolation and quantitative RT-PCR

Total RNA was extracted from frozen tissues using the RNeasy Plus Mini Kit (Qiagen), and cDNA was prepared from 2 µg RNA using the High Fidelity cDNA synthesis kit (Applied Biosystems/Roche). Quantitative RT-PCR analysis was performed on triplicate samples with SYBR green (Quantace) using the Rotor Gene 3000 (Corbett Research/Qiagen) over 40 cycles (94ºC/20s, 60ºC/15s, 72ºC/15s) and following an initial denaturation step at 95ºC/10min. The cDNA concentration of target genes was normalized by amplification of *18S rRNA* and fold changes in gene expression were obtained using the 2-ddCT method.

Histological quantification

Quantification of immunohistochemical stainings was performed using MetaMorph imaging software (Molecular Devices). The p-RPS6 and pY-STAT3 stainings on human GC biopsies were quantified by determining the proportion of the area positively stained for p-RPS6 or pY-STAT3 relative to the total biopsy area. Vascularization (microvessel area) and tissue hypoxia were quantified by determining the CD31-positive or hydroxyprobe-1-positive area relative to the total tissue area. Proliferation was enumerated by determining the number of BrdU-labelled cells per total tissue area.

GENE EXPRESSION PROFILING & ACTIVATION SCORES

Accession numbers

The array data are available at the NCBI Gene Expression Omnibus (GEO) repository (http://www.ncbi.nlm.nih.gov/projects/geo/): (I) Mouse gene expression profiles: GSE35808; (II) Human GC gene expression profiles, Singapore cohort: GSE15459, excluding eight profiles that either failed array quality control (GC-011LGE-T, GC-035PCC-T, GC-038LYC-T, GC-021LAH-T) or are not from gastric adenocarcinomas (GC-980327T, GC-2000619T, GC-026-GJK-T, GC-039-TSC-T); (III) Human GC gene expression profiles, Australia cohort: GSE35809; and (IV) Gene expression profiles of PI3K-activated primary mammary epithelial cells: GSE12815.

Calculating human GP130 activation scores by Bayesian Factor Regression Modelling (BFRM)

BFRM (5) uses a latent factor model in which the factor loadings matrix is sparse. Therefore, the latent factor is related to a relatively small number of genes that are related to a specific input gene signature (i.e. the human GP130 gene signature). Hence, BFRM can discover the main latent factor which corresponds to the underlying biological structures responsible for a specific gene signature. In the BFRM regression, the human GP130 gene signature was used as the seed gene set and constrained the maximum number of latent factors to one. We took the latent factor (*F*) as the magnitude of the GP130 activation score. The latent factors were then transformed to robust Z-scores by standardizing to a median of 0 and a median absolute deviation of 1. We used the probability quantile of the Z-score as the GP130 activation score. The sign of the GP130 activation score was determined by the factor loadings (*A*), specifically: Sign(GP130 activation score) = Sign(sum(*A*[up-regulated probe-sets]) - sum(*A*[down-regulated probe-sets]).

Derivation of the human PI3K gene signature and correlation with GC gene expression profiles

We derived a PI3K pathway activation signature from publically available array data (GEO: http://www.ncbi.nlm.nih.gov/geo; GSE12815). In this dataset, recombinant adenoviruses were used to express the p110α isoform of PI3K or a GFP control construct in primary mammary epithelial cells. RNA was then isolated from 8 independent PI3K-transduced lines and 11 GFP-transduced control lines and was profiled on Affymetrix HGU133 Arrays (6). Microarray data were preprocessed by Robust Multiarray Average normalization using the R Bioconductor (http://www.bioconductor.org/) “affy” package. LIMMA (7) was used to derive a human PI3K gene signature consisting of probes that represent differentially expressed genes between activated PI3K cells and GFP control cells (absolute fold change > 2 and FDR<$1x10^{-5}$;

Table S2). As described above, BFRM (5) was employed to compute a PI3K activation score which was then correlated with the gene expression profiles of our GC datasets (Table S1).

ADDITIONAL CELL CULTURE PROCEDURES

Suppression of Stat3 activity

For siRNA-mediated Stat3 knock-down, 293T cells were transfected with scrambled or Stat3-specific siRNA (Santa Cruz #29493) at the indicated concentration. Cells were collected 72 hours after transfection and cell lysates were subjected to immunoblot analysis. For PI3K activity assays, 293T cells were either transfected with Stat3 siRNA alone or together with a plasmid encoding the EpoR/gp130^{F2} receptor (4) and were analysed 72 hours after transfection. Alternatively, to suppress Stat3 activity, 293T cells were transfected with 1 µg of a plasmid encoding a dominant-negative variant of Stat3 (DN-Stat3; 8) either alone or together with EpoR/gp130^{F2}. These cultures were then used for the described PI3K activity assay 48 hours after transfection.

Luciferase assay

293T cells were transfected with 1 µg of the Stat3-responsive construct APRE-Luciferase (9) either alone or together with 1 µg of DN-Stat3. The cells were stimulated with Hyper-IL6 (100 ng/ml) 48 hours after transfection and were processed on the following day using the Luciferase Reporter Assay Kit (Promega) as per the manufacturer's instructions. Luminescence was measured with a Lumistar Galaxy Luminometer (Dynatech Laboratories).

BaF3 cell cultures, transfection, stimulation and PI3K and Jak inhibition

The murine pro B cell line BaF3 stably expressing the human IL11 receptor alpha (BaF3^{hulL11R}) was a gift from CSL Pty Ltd (Melbourne, Australia). BaF3^{hulL11R} cells were cultured in T75 flask in RPMI-1640 (Gibco/Invitrogen) supplemented with 10% foetal calf serum (FCS, Gibco/Invitrogen) and 2 ng/ml recombinant mouse IL3 (gift from CSL Pty Ltd, Melbourne, Australia). Transient transfections were carried out using the Nucleofactor (Lonza) and the optimized Cell Line Nucleofector Kit V (Lonza) as per the manufacturer's instructions. Transfected cells were cultured for 48 hours to ensure robust plasmid expression. Following 3 hours of starvation in FCS-containing medium devoid of IL3, cultures were stimulated with either recombinant human IL11 (100 ng/ml), Hyper-IL6 (100 ng/ml) or Epo (50 U/ml) for the indicated times. Where indicated, cultures were pre-treated with the PI3K inhibitor LY294002 (25 µM, Cell Signaling) or the pan-Jak inhibitor AG490 (75 µM, Sigma) 60 min prior to cytokine stimulation.

Supplemental References

1. Becker C, Fantini MC, Neurath MF. High resolution colonoscopy in live mice. *Nat Protoc.* 2006;1(6):2900-2904.

2. Tebbutt NC, Giraud AS, Inglese M, et al. Reciprocal regulation of gastrointestinal homeostasis by SHP2 and STAT-mediated trefoil gene activation in gp130 mutant mice. *Nat Med.* Oct 2002;8(10):1089-1097.

3. Schmitz J, Dahmen H, Grimm C, et al. The cytoplasmic tyrosine motifs in full-length glycoprotein 130 have different roles in IL-6 signal transduction. *J Immunol.* Jan 15 2000;164(2):848-854.

4. Schaeffer M, Schneiderbauer M, Weidler S, et al. Signaling through a novel domain of gp130 mediates cell proliferation and activation of Hck and Erk kinases. *Mol Cell Biol.* Dec 2001;21(23):8068-8081.

5. Carvalho CM, Chang J, Lucas JE, Nevins JR, Wang Q, West M. High-Dimensional Sparse Factor Modeling: Applications in Gene Expression Genomics. *J Am Stat Assoc.* Dec 1 2008;103(484):1438-1456.

6. Gustafson AM, Soldi R, Anderlind C, et al. Airway PI3K pathway activation is an early and reversible event in lung cancer development. *Sci Transl Med.* Apr 7 2010;2(26):26ra25.

7. Smyth GK. Linear models and empirical bayes methods for assessing differential expression in microarray experiments. *Stat Appl Genet Mol Biol.* 2004;3:Article3.

8. Kaptein A, Paillard V, Saunders M. Dominant negative stat3 mutant inhibits interleukin-6-induced Jak-STAT signal transduction. *J Biol Chem.* Mar 15 1996;271(11):5961-5964.

9. Takeda T, Kurachi H, Yamamoto T, et al. Crosstalk between the interleukin-6 (IL-6)-JAK-STAT and the glucocorticoid-nuclear receptor pathway: synergistic activation of IL-6 response element by IL-6 and glucocorticoid. *J Endocrinol.* Nov 1998;159(2):323-330.